SLAC–PUB–5304
July 1990
(T/A)

STABILITY OF ORBITS IN NONLINEAR MECHANICS FOR FINITE BUT VERY LONG TIMES*

R. L. WARNOCK and R. D. RUTH
Stanford Linear Accelerator Center,
Stanford University, Stanford, CA 94309, USA

ABSTRACT

In various applications of nonlinear mechanics, especially in accelerator design, it would be useful to set bounds on the motion for finite but very long times. Such bounds can be sought with the help of a canonical transformation to new action-angle variables $(\mathbf{J}, \mathbf{\Psi})$, such that the action $\mathbf{J}$ is nearly constant while the angle $\mathbf{\Psi}$ advances almost linearly with the time. By examining the change in $\mathbf{J}$ during a time T_o from many initial conditions in the open domain Ω of phase space, one can estimate the change in $\mathbf{J}$ during a much larger time T, on any orbit starting in a smaller open domain $\Omega_o \subset \Omega$. A numerical realization of this idea is described. The canonical transformations, equivalent to close approximations to invariant tori, are constructed by an effective new method in which surfaces are fitted to orbit data. In a first application to a model sextupole lattice in a region of strong nonlinearity, we predict stability of betatron motion in two degrees of freedom for a time comparable to the storage time in a proton storage ring (10^8 turns).

1. Introduction

Tracking of single particles, by symplectic numerical integration of Hamilton's equations,[1] provides a direct approach to the study of orbit stability. Unfortunately, computational expense usually limits the time interval of tracking to values much less than the desired storage time of an accelerator beam, and sharply restricts the number of initial conditions that can be tested. Favorable results from tracking are

* Work supported by Department of Energy contract DE–AC03–76SF00515.

Invited talk at the Workshop on Nonlinear Problems in Future Particle Accelerators, Capri, Italy, April 19–25, 1990.

regarded as a necessary condition for a good storage ring design, but doubt remains about the sufficiency of such results.

We propose a method to derive definite information on long-term stability from short-term tracking of many orbits. The idea derives from the line of argument of the Nekhoroshev Theorem,[2–5] and depends on determination of an action variable $\mathbf{J}$ that is invariant to high accuracy in a certain region of phase space. The residual time variation of $\mathbf{J}$, stronger in some regions than in others, provides a sensitive indicator of unstable behavior.

Nekhoroshev's original argument gives an explicit formula for a lower bound on the time of stability. The bound increases exponentially as the strength of the nonlinear perturbation tends to zero. Although our method does not give an explicit formula, it does yield stability times of practical interest, under realistic conditions. By contrast, the Nekhoroshev estimate gives suitable stability times only for absurdly weak perturbations. It may be possible to improve the Nekhoroshev estimates in simple examples,[6] but sufficient improvement for the complicated Hamiltonians of accelerator physics is not to be expected.

We achieve results for realistic parameters by avoiding Nekhoroshev's perturbative analysis. Our nonperturbative method is necessarily numerical, and for that reason involves some loss of rigor. We shall try to convince the reader that the results can nevertheless be highly reliable for the chosen Hamiltonian. Uncertainties in choosing the Hamiltonian are far greater than any ambiguity due to our technique.

In this brief account we describe only the main ideas, referring the reader to Ref. 7 for details of technique. We begin with the action-angle variables of the underlying linear system, $(\mathbf{I}, \mathbf{\Phi})$. Bold-faced symbols represent $d-$dimensional vectors, where d is the number of mechanical degrees of freedom. We treat an example with $d = 2$, but the method is general. Our discussion is based entirely on the time evolution map $\mathcal{M}$ for N_o turns,

$$\mathcal{M}: \quad (\mathbf{I}, \mathbf{\Phi})_{\theta=0} \mapsto (\mathbf{I}, \mathbf{\Phi})_{\theta=2\pi N_o} \ , \tag{1}$$

where $\theta = s/R$ represents azimuthal location on a closed reference orbit. In the present work we evaluate this map through element-by-element tracking. With sufficient care it should be possible to represent the map by an explicit formula, and thereby enhance the speed of calculations.[8,9]

A canonical transformation to new action-angle variables, $(\mathbf{I}, \mathbf{\Phi}) \mapsto (\mathbf{J}, \mathbf{\Psi})$, is induced by a generating function $G(\mathbf{J}, \mathbf{\Phi}, \theta)$ that is $2\pi-$periodic in $\mathbf{\Phi}$ and θ. The equations relating old and new variables are

$$\mathbf{I} = \mathbf{J} + G_{\mathbf{\Phi}}(\mathbf{J}, \mathbf{\Phi}, \theta) \ , \tag{2}$$

$$\mathbf{\Psi} = \mathbf{\Phi} + G_{\mathbf{J}}(\mathbf{J}, \mathbf{\Phi}, \theta) \ , \tag{3}$$

where subscripts denote partial derivatives. It is sufficient for our purposes to consider the transformation at $\theta = 0$ only. If the transformation is ideal, so that $\mathbf{J}$ is constant, then Eq. (2) gives an explicit representation of an invariant surface (a torus). That is, it gives $\mathbf{I}$ as a $2\pi-$periodic function of $\mathbf{\Phi}$. The invariant action $\mathbf{J}$

plays the role of a parameter to distinguish different tori; it is equal to the average of $\mathbf{I}$ over $\mathbf{\Phi}$. At $\theta = 0$ we adopt the notation

$$\mathbf{u}(\mathbf{J}, \mathbf{\Phi}) = G_{\mathbf{\Phi}}(\mathbf{J}, \mathbf{\Phi}, 0) \quad . \tag{4}$$

For the nonintegrable systems of interest, exact invariant tori exist, if at all, only for values of $\mathbf{J}$ on a strange set of Cantor type. Nevertheless, tori that are approximately invariant exist as smooth functions of $\mathbf{J}$ in open regions of phase space, and they can be computed numerically. A family of approximate invariant tori defines a canonical transformation. If $\mathbf{u}(\mathbf{J}, \mathbf{\Phi})$ is a smooth function of $\mathbf{J}$ in a region Ω, and

$$\mathbf{I}(\theta) \approx \mathbf{J} + \mathbf{u}(\mathbf{J}, \mathbf{\Phi}(\theta)) \ , \quad \theta = 0, 2\pi, 4\pi, \cdots \ , \tag{5}$$

then the equation $\mathbf{I} = \mathbf{J} + \mathbf{u}(\mathbf{J}, \mathbf{\Phi})$ defines a nearly constant function $\mathbf{J}(\mathbf{I}, \mathbf{\Phi})$. Here we assume that the Jacobian matrix $\mathbf{1} + \mathbf{u_J}(\mathbf{J}, \mathbf{\Phi})$ is nonsingular in the region of interest. It is indeed found to be nonsingular in our calculations. Integrating $\mathbf{u}$ with respect to $\mathbf{\Phi}$, we obtain the generator $G(\mathbf{J}, \mathbf{\Phi}, 0)$ and all the ingredients of a full canonical formalism. The function $\mathbf{u}(\mathbf{J}, \mathbf{\Phi})$, representing a family of approximate invariant tori, is constructed numerically by the method of Sec. 3.

2. A Bound on the Change in J

In a case with $d = 2$, let Ω be the interior of a rectangle in the $\mathbf{J} = (J_1, J_2)$ plane, and let Ω_o be the interior of a smaller, concentric rectangle so that $\Omega_o \subset \Omega$. Denote by ΔJ_i the width of the annulus between Ω_o and Ω as crossed in the ith direction. Suppose that the change in J_i during N_o turns, for any orbit with initial $\mathbf{J}$ in Ω, is less than δJ_i. Then any orbit with initial $\mathbf{J}$ in the smaller region Ω_o cannot reach the outer boundary of Ω in fewer than $N = qN_o$ turns, where

$$q = \min_i \left(\frac{\Delta J_i}{\delta J_i} \right) \quad . \tag{6}$$

This observation is useful if q is sufficiently large. Since the largest tolerable excursion ΔJ_i is sharply restricted by design considerations, a large q is to be achieved by making δJ_i small through a good choice of the canonical transformation.

Note that for practical purposes this is an extremely conservative argument, since it comes from contemplating the worst conceivable case in which the increment of J_i in qN_o turns is just q times the largest possible increment in N_o turns. In reality, the q increments are not likely to add up linearly, so that it will probably take much more than qN_o turns to move from Ω_o to the outer boundary of Ω.

3. Numerical Determination of the Canonical Transformation

To determine the canonical transformation, we expand the function representing a torus in a Fourier series. We write

$$\mathbf{I} = \sum_{\mathbf{m}} \mathbf{u_m} e^{i\mathbf{m}\cdot\mathbf{\Phi}} \ , \tag{7}$$

and determine the coefficients $\mathbf{u_m}$ so that Eq. (7) is satisfied at points $(\mathbf{I}(\theta), \mathbf{\Phi}(\theta))$, $\theta = 0 \ (mod\ 2\pi)$, all lying on a single nonresonant orbit. The coefficient $\mathbf{u_o}$ of the constant term is identified with the action $\mathbf{J}$, which varies with the choice of initial condition of the orbit. We repeat the process for various initial conditions, thereby obtaining $\mathbf{u_m(J)}$ on a mesh of points $\mathbf{J} = \mathbf{J}_i, \quad i = 1, 2, \cdots, s$. We then define $\mathbf{u_m(J)}$ as a smooth function of $\mathbf{J}$ by interpolating the values at mesh points with polynomials. The resulting transformation, $\mathbf{I} = \mathbf{J} + \mathbf{u}(\mathbf{J}, \mathbf{\Phi})$, is mathematically well defined, even though it was obtained numerically.

In determining the $\mathbf{u_m}$ to satisfy Eq. (7), we face the difficulty that the $\mathbf{\Phi}(\theta)$ are scattered unpredictably. For that reason we cannot simply take a discrete Fourier transform, which requires regularly spaced abscissae. Furthermore, a direct solution of the linear equations for the $\mathbf{u_m}$ is impractical, since the matrix is dense and too large for comfort. We avoid these problems by using the values of $\mathbf{I}$ on a regular mesh in $\mathbf{\Phi}$ space as unknowns, rather than the $\mathbf{u_m}$. In one dimension the equations relating values of I at orbit points ϕ_j to values at mesh points $2\pi k/K$ are as follows:

$$I(\phi_j) = \sum_{k=0}^{K-1} D_{jk}\ I(2\pi k/K) \quad , \tag{8}$$

where

$$D_{jk} = \frac{\sin[\pi(x_j - k)]}{K \sin[\pi(x_j - k)/K]} \quad , \tag{9}$$

with

$$\phi_j = 2\pi x_j / K \quad . \tag{10}$$

Here $K = 2M + 1$, where M is the maximum mode number m. To derive these equations, one substitutes in Eq. (7) the approximation to $\mathbf{u_m}$ that is given by the discrete Fourier transform. Reversal of the order of summations, and evaluation of a geometric series, leads to Eq. (8). This system can be solved by iteration provided that we choose to fit only a subset of the data, namely, a set in which there is one and only one ϕ_j in each cell of the mesh. With this selection the matrix D_{jk} is close to the unit matrix, and an iterative method (Gauss-Seidel) converges rapidly. Using the inverse of the discrete Fourier transform, we finally obtain the torus in the form Eq. (7).

This method has three notable properties. First, the resulting torus Eq. (7) passes exactly through the orbit points, provided that the Eq. (8) is solved exactly. This feature may be partly responsible for the high accuracy of the method. Second, the scheme works in any number of dimensions. Third, it provides a useful filter against low-order resonances. In the case of resonant orbits of sufficiently low order, the process of selecting data will fail. Not every cell of the mesh will contain a $\mathbf{\Phi}(\theta)$, no matter how long the orbit, and the iterative solution of Eq. (8) will fail. We fit only nonresonant orbits (invariant tori) or resonant orbits of extremely high order (which are not distinguishable numerically from tori). In Fig. 1 we plot values of $\mathbf{\Phi}$ on a typical resonant orbit. Figure 2 shows values of $\mathbf{\Phi}$ on an apparent invariant

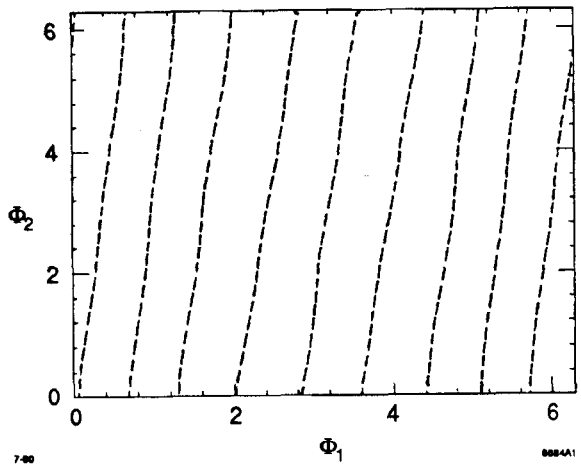

Figure 1: Values of $\Phi = (\Phi_1, \Phi_2)$ at the surface of section $\theta = 0$ on a resonant orbit.

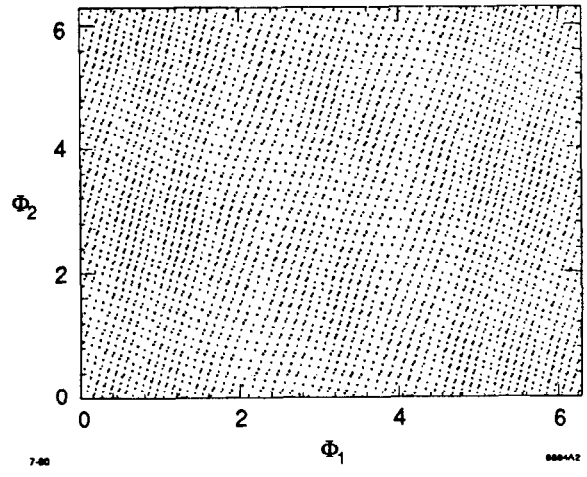

Figure 2: Values of $\Phi = (\Phi_1, \Phi_2)$ at the surface of section $\theta = 0$ on an apparent invariant torus.

torus. Figure 3 shows points on a nonresonant orbit, at $\theta = 0 \ mod(2\pi)$, plotted in three dimensions. We plot (I_1, Φ_1, Φ_2), with I_1 on the vertical axis. If the motion were linear these points would lie in a plane, $I_1 = constant$.

The polynomial interpolation in $\mathbf{J}$ of the tori forms bridges over resonances. Since there are resonances everywhere, this is an essential feature of any canonical transformation defined as a smooth function of $\mathbf{J}$. It is not merely a feature forced upon us by the use of numerical methods.

4. Computation of δJ_i

To compute a bound it remains to determine δJ_i. Because of practical limits on computation time, there is some uncertainty in this determination, but with some care the uncertainty can be made rather small. It should be emphasized that the

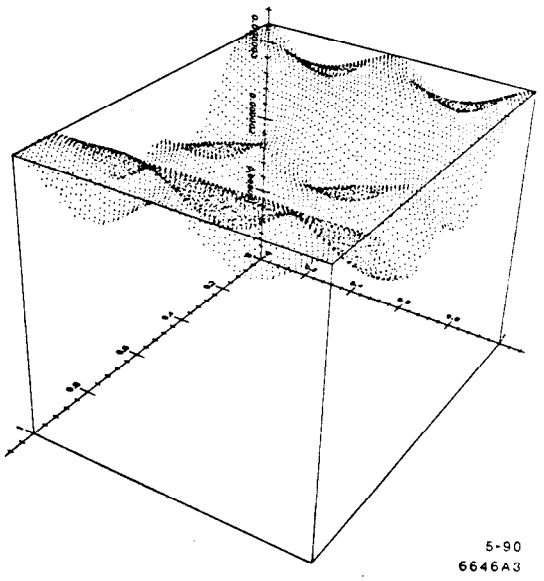

Figure 3: Plot of I_1 (on the vertical axis) versus Φ_1 and Φ_2, for a torus in the region Ω defined in Eq. (13). The origin is at $I_1 = 0$.

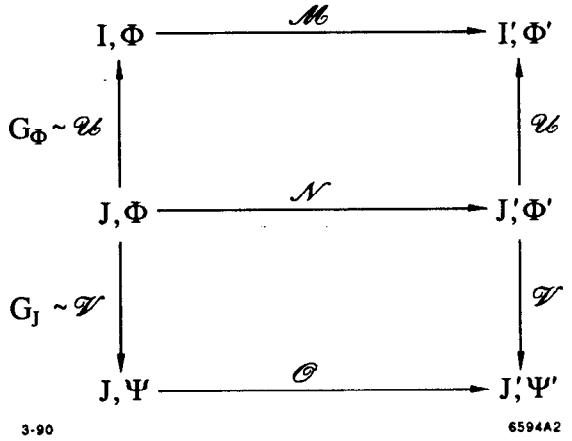

Figure 4: A commutative diagram showing how the maps $\mathcal{N}$ and $\mathcal{O}$ are induced by the original map $\mathcal{M}$ and changes of variable. The transformations $\mathcal{U}$ and $\mathcal{V}$ are given in explicit form through derivatives of the generator; see Eqs. (2) and (3).

only failure of rigor in our argument occurs in the determination of δJ_i.

We denote the increment in $\mathbf{J}$ over N_o turns as

$$\mathbf{J}' - \mathbf{J} = \mathcal{D}(\mathbf{J}, \mathbf{\Phi}, N_o) \quad . \tag{11}$$

To compute $\mathcal{D}$ we simply observe the time evolution of $\mathbf{J}$ induced by the map $\mathcal{M}$ through the change of variable $\mathcal{U} : (\mathbf{J}, \mathbf{\Phi}) \mapsto (\mathbf{I}, \mathbf{\Phi})$ and its inverse. Here we need not be concerned with the time evolution of the new angle $\mathbf{\Psi}$. It is enough to deal with the mixed pair $(\mathbf{J}, \mathbf{\Phi})$, which evolves by a map $\mathcal{N}$:

$$\mathcal{N} : (\mathbf{J}, \mathbf{\Phi}) \mapsto (\mathbf{J}', \mathbf{\Phi}') \quad . \tag{12}$$

The commutative diagram of Fig. 4 shows how $\mathcal{N}$ is obtained as $\mathcal{N} = \mathcal{U}^{-1} \circ \mathcal{M} \circ \mathcal{U}$. For the computation of $\mathcal{N}$ we have $\mathcal{U}$ in explicit form, since $\mathbf{I} = \mathbf{J} + \mathbf{u}(\mathbf{J}, \mathbf{\Phi})$. To evaluate $\mathcal{U}^{-1}$ we use Newton's method, with $\mathbf{J}$ as the first guess for $\mathbf{J}'$. The first iterate of Newton's method already provides accuracy that is more than adequate for our purposes.

The map $\mathcal{O}$ on the new canonical pair $(\mathbf{J}, \mathbf{\Psi})$, shown in the third level of Fig. 4, is needed only for the work of Sec. 6. For the computation of $\mathcal{O}$ we have $\mathcal{V}$ in explicit form through Eq. (3), but $\mathcal{V}^{-1}$ must be calculated by Newton's method.

In the example studied below, the function $\mathcal{D}$ has many oscillations as a function of $\mathbf{\Phi}$ but relatively few as a function of $\mathbf{J}$ on Ω. It is impractical to follow every oscillation in seeking the upper bound δJ_i of $\mathcal{D}_i$, but we can do random sampling with statistical estimates of sampling error to find a fairly convincing value of δJ_i. The reader may consult Ref. 7 for details on this relatively delicate problem.

5. An Example

To illustrate, we derive a bound for two-dimensional betatron motion in a lattice consisting of one cell of the Berkeley Advanced Light Source (ALS). The lattice parameters are given in Ref. 7. This example involves nonlinear phenomena similar to those in large hadron colliders since the sextupoles are so strong as to drive high-order resonances such as those excited by high-order multipoles in superconducting magnets. We work in a region Ω of substantial nonlinearity, about half-way to the short-term dynamic aperture in the (x_{max}, y_{max}) plane. Orbit points on a typical invariant surface in this region are plotted in Fig. 3. With actions measured in meters the region Ω is given by

$$2.51 \cdot 10^{-6} \text{ m} < J_1 < 2.82 \cdot 10^{-6} \text{ m}\,, \quad 1.34 \cdot 10^{-6} \text{ m} < J_2 < 1.64 \cdot 10^{-6} \text{ m}\,. \tag{13}$$

We first determine the leading resonances in this region with the help of our canonical formalism. The tune $\boldsymbol{\nu}$ (winding number) is obtained as a function of $\mathbf{J}$ from Eq. (3). If $\mathbf{J}$ were constant, then the change in $\mathbf{\Psi}$ over one turn would be equal to $2\pi\boldsymbol{\nu}$, and Eq. (3) would give

$$2\pi\boldsymbol{\nu}(\mathbf{J}) = \mathbf{\Phi}(2\pi) - \mathbf{\Phi}(0) + G_{\mathbf{J}}(\mathbf{J}, \mathbf{\Phi}(2\pi), 0) - G_{\mathbf{J}}(\mathbf{J}, \mathbf{\Phi}(0), 0)\ . \tag{14}$$

We take this equation to define $\boldsymbol{\nu}(\mathbf{J})$, even when $\mathbf{J}$ is not precisely constant. It is easy to construct the inverse function $\mathbf{J}(\boldsymbol{\nu})$ by an interpolation technique described in Ref. 7. This function serves to map the resonant tune lines, $m_1\nu_1 + m_2\nu_2 = n$, into the $\mathbf{J}$ plane. Figure 5 shows all resonances in the region Ω of the $\mathbf{J}$ plane with $|m_i| \leq 20$. The stars indicate the mesh points $\mathbf{J}_i$ used to set up the canonical transformation as a smooth function of $\mathbf{J}$. The transformation as represented in Eq. (7) includes up to 20 Fourier modes in each angle Φ_i.

We verify that this method accurately locates resonances in the $\mathbf{J}$-plane, even in the case of narrow resonances of high order. For instance, we follow an orbit by tracking, taking an initial condition on the (17,16) line of Fig. 5. Plotting

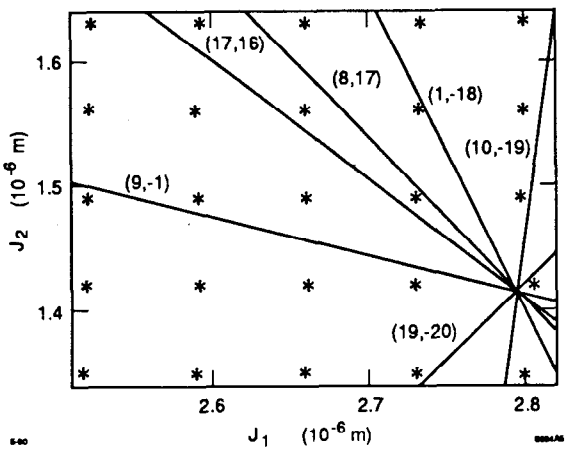

Figure 5: The image in the (J_1, J_2) plane of all resonance lines $m_1\nu_1 + m_2\nu_2 = n$ with $|m_i| \leq 20$, for the region Ω defined in Eq. (13). Each line is labeled by (m_1, m_2). The stars indicate the mesh points $\mathbf{J}_i$ used to set up the canonical transform as a smooth function of $\mathbf{J}$.

Table 1: Data on $\mathbf{J}' - \mathbf{J} = \mathcal{D}(\mathbf{J}, \mathbf{\Phi}, N_o)$, the change of $\mathbf{J}$ in N_o turns, for 400 random samples of $(\mathbf{J}, \mathbf{\Phi})$ with $\mathbf{J}$ in subregion Ω_4 as defined in Ref. 7. The brackets <> indicate ensemble averages.

N_0	$\max\|\mathcal{D}_1\|$	$\max\|\mathcal{D}_2\|$	$<\|\mathcal{D}_1\|>$	$<\|\mathcal{D}_2\|>$	$<\mathcal{D}_1>$	$<\mathcal{D}_2>$
1	$9.9 \cdot 10^{-13}$	$1.9 \cdot 10^{-12}$	$2.4 \cdot 10^{-13}$	$4.7 \cdot 10^{-13}$	$3.8 \cdot 10^{-15}$	$-6.4 \cdot 10^{-15}$
10	$1.5 \cdot 10^{-12}$	$1.7 \cdot 10^{-12}$	$2.7 \cdot 10^{-13}$	$4.7 \cdot 10^{-13}$	$2.1 \cdot 10^{-15}$	$3.8 \cdot 10^{-14}$
100	$1.2 \cdot 10^{-12}$	$2.5 \cdot 10^{-12}$	$3.1 \cdot 10^{-13}$	$5.4 \cdot 10^{-13}$	$-2.7 \cdot 10^{-14}$	$-2.0 \cdot 10^{-14}$
1000	$1.5 \cdot 10^{-12}$	$2.7 \cdot 10^{-12}$	$3.3 \cdot 10^{-13}$	$5.2 \cdot 10^{-14}$	$1.3 \cdot 10^{-14}$	$2.7 \cdot 10^{-14}$
10000	$1.9 \cdot 10^{-12}$	$2.7 \cdot 10^{-12}$	$4.0 \cdot 10^{-13}$	$6.5 \cdot 10^{-13}$	$1.0 \cdot 10^{-14}$	$3.9 \cdot 10^{-14}$

$\Phi(\theta)$, $\theta = 0, 2\pi, 4\pi, \cdots$, we see apparent curves in the (Φ_1, Φ_2) plane, having 17 intersections with the Φ_1 axis and 16 with the Φ_2 axis; (actually, these are resonant structures of nonzero width, not curves).

Turning now to the computation of δJ_i in the region Ω, we show in Table 1 some typical results for the deviations $\mathcal{D}_i$ of Eq. (11). The results are for a subregion Ω_4 of Ω, roughly one fourth of the full region, and correspond to an ensemble from 400 random samples of $(\mathbf{J}, \mathbf{\Phi})$, $\mathbf{J} \in \Omega_4$, $\Phi_i \in [0, 2\pi]$. The table shows the ensemble maximum of $|\mathcal{D}_i|$, the ensemble average of the same, and the ensemble average of $\mathcal{D}_i$ including sign. It is remarkable that each of these quantities has the same order of magnitude at all N_o up to 10^4. Recalling Eq. (13), we see that $\mathbf{J}$ is constant to about one part in 10^6 for at least 10^4 turns. Moreover, the orbit follows a torus to still greater accuracy in some average sense: the ensemble average of $\mathcal{D}_i$ including sign is considerably smaller than the average absolute value.

The discussion of Ref. 7 yields the following values for the numbers δJ_i that bound $\mathcal{D}_i$, for $N_o = 10^4$:

$$(\delta J_1, \delta J_2) = (2.8, 4.0) \cdot 10^{-12} \text{ m} \ . \tag{15}$$

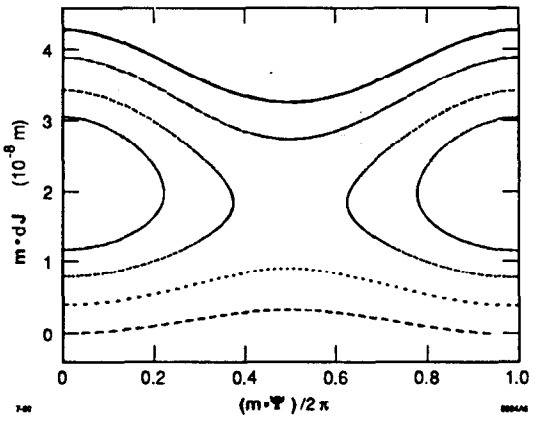

Figure 6: Pseudopendulum motion of the angle-action pair $(\mathbf{m}\cdot\mathbf{J}, \mathbf{m}\cdot\boldsymbol{\Psi})$ near a $(5,6)$ resonance. Here $\mathbf{m}\cdot\boldsymbol{\Psi}$ is plotted modulo 2π.

The corresponding values for $N_o = 10^k$, $k = 0,1,2,3,4$, have similar magnitudes. Let us choose ΔJ_i of Sec. 2 so that $q = \Delta J_i/\delta J_i = 10^4$, with $N_o = 10^4$. Then the subset Ω_o of Ω is defined by

$$2.54\cdot 10^{-6}\ \mathrm{m} < J_1 < 2.79\cdot 10^{-6}\ \mathrm{m}\ , \quad 1.38\cdot 10^{-6}\ \mathrm{m} < J_2 < 1.60\cdot 10^{-6}\ \mathrm{m}\ . \quad (16)$$

Any orbit beginning in Ω_o will stay within the slightly larger region Ω for at least $qN_o = 10^8$ turns.

6. Effect of a Strong Resonance

All resonances in the region Ω defined above are weakly excited, and have little effect. The variation of $\mathbf{J}$ on the resonance lines is hardly stronger than elsewhere in the region. In other regions, at comparable amplitudes, we encounter strong resonances that are associated with larger variations of $\mathbf{J}$. This does not necessarily imply a degradation of the time for stability, since oscillations on a well isolated resonance can be stable and not associated with fast transport to nearby resonances, even if the amplitude of oscillation is fairly large. We have studied one such resonance, with $(m_1, m_2) = (5,6)$. In the vicinity of this resonance, the variables $(\mathbf{J}, \boldsymbol{\Psi})$ follow approximately the pattern expected of action-angle variables in the isolated resonance model.[10] That is to say, $m_2J_1 - m_1J_2$ is nearly constant, while $\mathbf{m}\cdot\mathbf{J}$ and $\mathbf{m}\cdot\boldsymbol{\Psi}$ behave as action and angle of a physical pendulum. The phase portrait of the latter variables is shown in Fig. 6, with $\mathbf{m}\cdot\boldsymbol{\Psi}$ plotted modulo 2π.

To establish long-term stability in this situation, we have to limit any movement in the center of oscillation of the pendulum, for any initial condition in the region considered. That can be done by limiting separately the changes parallel to $\mathbf{m}$ and perpendicular to $\mathbf{m}$. For the latter, one can merely put a bound on the change of $m_2J_1 - m_1J_2$, as in our previous bounds on the change of $\mathbf{J}$. For the former, we examine the pendulum motion beyond the separatrix, where full rotations of the pendulum, rather than librations, occur. If the apparent rotation curves of

Fig. 6 behaved like K.A.M. curves of a system in $1\text{-}\frac{1}{2}$ degrees of freedom, they would permanently confine the motion of $\mathbf{m} \cdot \mathbf{J}$. Actually, the apparent curves are not really curves, as inspection on a finer scale reveals. The motion of $\mathbf{m} \cdot \mathbf{J}$ follows a curve within an accuracy of about 10^{-11} m, however, for several thousand turns. This is entirely analogous to the situation of the previous section in which $\mathbf{I}$ follows a two-dimensional torus to a certain accuracy. Consequently, we can proceed in the same way as before, by finding a continuous family of curves that fit the motion to high accuracy, then bounding uniformly the deviation from a curve during N_o turns. We have not yet carried out such a formal program. On the basis of informal estimates, we predict stability in a region Ω_r containing the $(5, 6)$ resonance for at least 10^7 turns.

7. Conclusion

We have described a method for theoretical prediction of orbit stability over times comparable to storage times in hadron rings. With further development the method should become practical for machine design. It uses calculational methods that are feasible for elaborate models of large machines, provided that the speed of tracking can be increased substantially. We think that there are good prospects of achieving the necessary speed through construction of full turn maps. Indeed, the preliminary work of Ref. 8 already indicates that very accurate maps can be constructed in a straightforward way.

REFERENCES

1. É. Forest and R. D. Ruth, *Physica D* **43** (1990) 105.
2. N. N. Nekhoroshev, *Russian Math. Surveys* **32**:6 (1977) 1.
3. G. Benettin, L. Galgani, and A. Giorgilli, *Celestial Mech.* **37** (1985) 1.
4. G. Benettin, in *Nonlinear Evolution and Chaotic Phenomena*, eds. G. Gallavotti and P. F. Zweifel, (Plenum, New York, 1988).
5. A. Bazzani, S. Marmi, and G. Turchetti, "Nekhoroshev Estimate for Isochronous Nonresonant Symplectic Maps," University of Bologna preprint, 1990.
6. P. Lochak and A. Porzio, *Ann. Inst. H. Poincaré*, **51** (1989) 199.
7. R. L. Warnock and R. D. Ruth, "Long-Term Bounds on Nonlinear Hamiltonian Motion," SLAC–PUB–5267; submitted to *Physica D.*
8. R. L. Warnock, *Proc. 1989 IEEE Part. Accel. Conf.*, p. 1322. In Table 1 of this paper, the second entry in the second column should have exponent -7.
9. J. Irwin, Superconducting Supercollider report SSC–228.
10. L. Michelotti, *AIP Conference Proceedings* **184**, Vol. 1, *Physics of Particle Accelerators* (Amer. Inst. Phys., New York, 1989).